Nonchaotic laser pulse dissociation through deformed tori

Emanuel F. de Lima [*]

Departamento de Física, Universidade Federal de São Carlos São Carlos SP 13565-905, Brazil

R. Egydio de Carvalho[†] and M. D. Forlevesi[‡]

Universidade Estadual Paulista (UNESP) Instituto de Geociências e Ciências Exatas-IGCE Rio Claro SP 13506-900, Brazil

We consider the nonlinear classical dynamics of a diatomic molecule under the action of a laser field in the framework of the driven Morse oscillator model. We investigate the influence of the dipole function and the laser field on the deformations of the surviving, invariant tori. For intense and high-frequency fields, some invariant tori traverse the separatrix of motion, visiting both the bound and unbound regions of the interatomic potential. Based on this fact, we propose the use of appropriately designed laser pulses to induce dissociation of trajectories on such invariant tori. This mechanism constitutes a controlled nonchaotic route for dissociation, which is an alternative to chaotic multiphoton dissociation and to chirped pulse dissociation.

I. INTRODUCTION

The study of chaotic systems has proved to be important for many branches of physics, including the control of the dynamics of atoms and molecules by external time-dependent fields [1,2]. The onset of chaotic motion, marked by the extreme sensitivity of the dynamics to the initial conditions, is the starting point for many investigations. For instance, the classical ionization of atoms and dissociation of molecules by single-frequency fields are often recognized to occur through chaotic routes [3–5]. Nevertheless, it is well known that invariant surfaces, the so-called KAM tori, may continue to exist for dynamical systems perturbed away from integrable ones. As we show here, the study of the deformations of invariant surfaces can be important for implementing control mechanisms for chaotic systems.

Along with the kicked rotor and the one-dimensional (1D) hydrogen atom, the Morse oscillator is a fundamental model for understanding chaotic behavior of atoms and molecules under the action of time-dependent fields. The classical driven Morse oscillator has been extensively applied to the study photodissociation of diatomic molecules [6–13]. Several quantum-classical comparisons have also been carried out, and it is generally agreed that there are some correspondences between quantum and classical results, especially far from multiphoton processes [14–23].

In the dipole approximation, the molecule-field interaction is given by the product of the dipole function and the time-dependent external field. Diatomic molecules possess diverse shapes for the dipole function, with distinct spatial ranges and, in some cases, presenting oscillatory behavior [24–27]. Previous works have investigated the influence of the shape of

dipole function on the dissociation dynamics and have found that it greatly impacts the dissociation probability [28,29]. However, the effects of the dipole function on the surviving tori have not been considered yet.

The classical free Morse oscillator has two distinct kinds of motions: bound motion (libration) in a finite low-energy range and unbound motion from an energy threshold up to infinity. This energy threshold corresponds to a separatrix of the two kinds of motion. The dipole coupling with an external single-frequency field may induce transitions between these two energy regions. A change in the dynamics from local chaos and quasiperiodicity to global chaos takes place as the intensity of the field increases. As a result, the trajectories can diffuse toward dissociation as the last bounding torus is broken [6,7]. An alternative to this single-frequency scheme for achieving dissociation is the use of chirped pulses: The initial trajectories are trapped in resonant-stability regions in phase space which can be dragged upward in energy by adiabatically chirping the field frequency [30,31]. Additionally, a method for population transfer in diatomic molecules by means of adiabatic rapid passage has also been considered [32,33]. Moreover, there is still other technique for controlling molecular systems not involving lasers in which an applied external electric field is made to vary at specific rates in order to make a desired transition [34].

It has been recently proposed a scheme to control photodissociation on the driven Morse model based on the existence of surviving tori, which cross the separatrix of motion [35]. It has been shown that there exist such invariant tori in the presence of intense and high-frequency fields. The trajectories trapped on such tori do not dissociate, although they reach energies above the dissociation threshold. Thus, by placing the initial trajectories on such tori the dissociation is inhibited.

In the present work, we consider nonlinear dynamics of a diatomic molecule under the presence of a harmonic laser field in the framework of the driven Morse oscillator. Extending the results of Ref. [35], we investigate the impact of the

---

[*]emanuel@df.ufscar.br

[†]ricardo.egydio@unesp.br

[‡]forlevesi@gmail.com

dipole function and of the external field parameters on the deformations of the surviving tori. Based on the existence of surviving tori which cross the separatrix of motion, we propose the use of laser pulses to induce dissociation of trajectories on such tori. To our knowledge, this dissociation mechanism has not been explored yet.

The paper is organized as follows: In Sec. II, a general treatment for the deformation of the surviving tori under external fields is presented. In this section, some results are obtained from perturbation theory, which help to understand the role of the diverse parameters of the interaction Hamiltonian in the tori deformations. In Sec. III, we consider the deformations of the surviving tori for the Morse oscillator, presenting numerical results obtained from directly solving the equations of motion. Section IV is devoted to show how external pulses can be devised to induced dissociation through nonchaotic routes. Finally, conclusions are drawn in Sec. V.

II. DEFORMATION OF SURVIVING TORI

Consider a one-dimensional system with Hamiltonian $H_0(x, p)$, which may represent a free atom or molecule. Consider also that the coupling of the system with an external field is given by the interaction Hamiltonian $H_1(x, t) = -\mu(x)\mathcal{E}(t)$, with $\mu(x)$ representing the dipole function of the system and an applied time-dependent external field $\mathcal{E}(t)$. In action-angle variables (J, θ), the total Hamiltonian can be written as

$$H(J, \theta, t) = H_0(J) + H_1(J, \theta, t). \tag{1}$$

For H_0 alone, the system is integrable and we have $J = J_0$, $\theta = \omega t + \theta_0$, and $\omega(J) = \frac{\partial H_0}{\partial J}$, with J_0, ω, and θ_0 independent of time.

We assume further that the field is given by $\mathcal{E}(t) = \epsilon \sin(\Omega t)$ and that the dipole can be written in a Fourier series in the angle variable such that the interaction Hamiltonian reads

$$H_1(J, \theta) = -\epsilon \sum_{n=0}^{\infty} [f_n(J) \cos(n\theta) + g_n(J) \sin(n\theta)] \sin(\Omega t),$$

$$\tag{2}$$

where the Fourier components are given by

$$f_0(J) = \frac{1}{2\pi} \int_0^{2\pi} \mu(J, \theta) d\theta, \tag{3}$$

$$f_n(J) = \frac{1}{\pi} \int_0^{2\pi} \mu(J, \theta) \cos(n\theta) d\theta, \tag{4}$$

$$g_n(J) = \frac{1}{\pi} \int_0^{2\pi} \mu(J, \theta) \sin(n\theta) d\theta, \tag{5}$$

with $g_0(J) \equiv 0$.

From the KAM theorem, it is known that in the presence of the perturbation H_1, invariant surfaces may continue to exist for some initial conditions. Let us assume that a surviving torus exists, such that the original Hamiltonian $\bar{H}(\theta, J, t)$ can be locally transformed to a new Hamiltonian $\bar{H}(\bar{J})$, which is a function of the new action $\bar{J}$ only. The corresponding canonical transformation implies that we can relate the old action

with the new action-angle variables, that is, $J = J(\bar{J}, \bar{\theta}, t)$, which can be written as

$$J = \bar{J} + \delta(\bar{J}, \bar{\theta}, t), \tag{6}$$

where δ is the term associated to the deviation from the original torus, which we call *deformation parameter*.

We may further restrict to a Poincaré section with $t = 2\pi k/\Omega$ (k integer), eliminating the time in the previous expression and writing

$$J_{\text{PS}} = \bar{J} + \delta_{\text{PS}}(\bar{J}, \bar{\theta}), \tag{7}$$

where the label PS refers to the values of the original action variable and deformation parameter in the Poincaré surface-of-section. Since a certain range in the old action J corresponds to a constant $\bar{J}$, the surviving torus covers a range in the energy of the unperturbed system $H_0(J)$. The excursion in energy in a surface-of-section of a given deformed torus can be defined as the difference between the maximum and minimum values of the unperturbed energy H_0 in that surface, i.e.,

$$\Delta_E = \max\{H_0(J_{\text{PS}})\} - \min\{H_0(J_{\text{PS}})\}, \tag{8}$$

where J_{PS} is calculated for a fixed $\bar{J}$ from Eq. (7). In Ref. [35] the quantity Δ_E is referred to as the *energy inclination*.

We note that the maximum and minimum values of H_0 as well as the corresponding energy inclination are of paramount importance for our controlling method of energy transitions, in particular dissociation, which is explored in Sec. IV. For a given set of external field parameters and a given dipole function, these quantities furnish the energy range covered by a deformed torus, and, as we shall see, transitions between two energies within this range can be induced by means of appropriately designed pulses.

In order to access the dependence of the deformation on the interaction Hamiltonian parameters, we have applied the canonical perturbation theory [36]. In order to avoid the small denominators, we assume that the field is off-resonance, meaning that the value of the initial action variable is sufficiently far from any nonlinear resonance $n\omega(J_n^{\text{res}}) - \Omega = 0$, with n being an integer J_n^{res} being the corresponding resonant value of the action. To first order on the field amplitude ϵ we have obtained

$$\delta_{\text{PS}}(\bar{J}, \bar{\theta}) \approx \epsilon \sum_{n=0}^{\infty} [-\lambda_n(\Omega, \bar{J}) \sin(n\bar{\theta}) + \sigma_n(\Omega, \bar{J}) \cos(n\bar{\theta})],$$

$$\tag{9}$$

with

$$\lambda_n(\Omega, \bar{J}) = \frac{n f_n(\bar{J}) \Omega}{\Omega^2 - n^2 \omega(\bar{J})^2}, \tag{10}$$

$$\sigma_n(\Omega, \bar{J}) = \frac{n g_n(\bar{J}) \Omega}{\Omega^2 - n^2 \omega(\bar{J})^2}. \tag{11}$$

Equations (10) and (11) show that for fixed amplitude of the external field, increasing values of the frequency of the external field tend to decrease the deformation of the tori and, consequently, decrease the energy inclination. Thus, regularization of the phase space with respect to tori deformation

is expected in the high-frequency regime. For very high-frequency fields, the deformation parameter depends essentially on the amplitude-frequency ratio ϵ/Ω and on the Fourier expansion of the interaction Hamiltonian. Consequently, surviving tori with large deformations may exist for intense and high-frequency fields. Moreover, if the unperturbed frequency $\omega(J)$ is a decreasing function of the action, in the high-frequency regime, $\Omega > \omega(J)$, then the resonance condition will only be met for large values of n. Usually $|f_n(J)|$ and $|g_n(J)|$ decrease with n, and, consequently, nonlinear resonances can be easily avoided. This situation should hold for systems such as the one-dimensional hydrogen atom and the Morse oscillator [37]. We note further that the dependence of the deformation with the dipole function occurs through the Fourier components $f_n(\bar{J})$ and $g_n(\bar{J})$.

III. THE DRIVEN MORSE OSCILLATOR

Consider the Hamiltonian of the driven Morse oscillator given by H_0, representing the molecular Hamiltonian in the absence of external fields and by H_1 representing the field-molecule interaction [35]. The Hamiltonian H_0 can be written as

$$H_0 = \frac{p^2}{2} + \frac{1}{2}(e^{-2x} - 2e^{-x}), \tag{12}$$

For convenience, dimensionless variable are considered here. The connection with molecular parameters can be found, e.g., in Ref. [28]. The energy range for bound motion (libration) is $-0.5 < E < 0$, and unbound motion is set for positive energies $E > 0$, with a separatrix at $E = 0$.

As in the previous section, the interaction of the oscillator with a harmonic field is given by

$$H_1 = -\mu(x)\mathcal{E}(t) = -\mu(x)\epsilon \sin \Omega t, \tag{13}$$

with $\mu(x)$ being the dipole function. We consider a dipole function depending on three parameters, ξ, η, and x_e,

$$\mu(x, \xi, \eta) = \frac{\sin[\eta(x + x_e)]}{\eta} \exp[-\xi(x + x_e)^4], \tag{14}$$

where η sets the oscillatory behavior, ξ sets the spatial range, and x_e sets an overall displacement of the dipole. For $\eta \to 0$, $\xi = 0.0029$, and $x_e = 2.135$ the dipole corresponds to that of the HF molecule [38]. The shape of the permanent dipole of many diatomic molecules can be approximated by adjusting these parameters [25]. Here, we will focus on the η and ξ parameters, setting $x_e = 2.135$.

In action-angle variables (J, θ) the total Hamiltonian for $E < 0$ becomes [7,39]

$$H = H_0(J) - \epsilon\mu(x(J, \theta), \xi, \eta)\sin(\Omega t), \tag{15}$$

where

$$H_0(J) = -\frac{1}{2}(1 - J)^2 \tag{16}$$

and [7]

$$x(J, \theta) = \ln\left[\frac{1 + \sqrt{2J - J^2}\cos\theta}{(1 - J)^2}\right]. \tag{17}$$

The action for bound motion corresponds to the interval $0 \leqslant J < 1$ and the unperturbed frequencies are given by

$\omega(J) = 1 - J$. Note that $H_0(J)$ is a monotonically increasing function of J in the bound region. The deformation parameter to first order in ε is given by Eq. (9) setting the σ_n terms to zero (since the dipole is an even function of θ). All the results presented in the subsequent figures were obtained by direct numerical integration of the equations of motion.

Figure 1 shows the energy inclination Δ_E and the maximum value of H_0 as a function of the dipole range parameter ξ in the Poincaré section defined by $t = 2\pi k/\Omega$ (k integer). The energy of the initial conditions was set to $E = -0.162$ (corresponding to the $\nu = 9$ level of HF) and the angle variable was set to $\theta = 0$. Figure 1(a) shows that the energy inclination decreases for increasing frequency (fixed amplitude $\epsilon = 1.6$), while Fig. 1(c) shows that the inclination increases for larger amplitudes (fixed frequency $\Omega = 9$). The blue, red, and black curves on these panels have the same ϵ/Ω ratio and show the agreement with the perturbative analyses of Sec. II. The behavior of the inclination with the dipole range parameter ξ is quite interesting: It presents a minimum close to $\xi = 0.009$, the inclination being large either for long-range dipoles $\xi \to 0$ and for short-range dipole, e.g., $\xi = 0.04$. Figures 1(b) and 1(d) show that the invariant tori can reach energies above the separatrix of the free motion $H_0 = 0$ for some value of ξ, especially in the case of high ϵ-Ω ratio.

As in the previous figure, Fig. 2 shows the energy inclination Δ_E and the maximum value of H_0 but now as a function of the dipole oscillation parameter η in the Poincaré section defined by $t = 2\pi k/\Omega$ (k integer). The dependence of the energy inclination on the field parameters is essentially the same obtained in Fig. 1, whereas the behavior of the inclination with the dipole parameter η is oscillatory. Interestingly, the inclination is quite large for a highly oscillatory dipole, e.g., for $\eta = 3.25$, although the magnitude of such dipole is comparatively smaller than for $\eta = 0$ [see Eq. (14)]. Again, Figs. 1(b) and 1(d) show that the invariant tori can reach energies above the separatrix of the free motion $H_0 = 0$ for some value of η, especially in the case of high ϵ-Ω ratio.

Figure 3 compares the behavior of the energy inclination as a function of the dipole parameters for three distinct initial energies. Figure 3(a) shows the inclination versus ξ, while Fig. 3(b) shows the inclination versus η. Two main aspects can be noted: (i) increasing the initial energy leads to a increasing of the energy inclinations and (ii) changing the dipole parameter leads to a small shift of the energy inclination curves.

Figure 4 shows the stroboscopic map (red dots) for a set of trajectories with initial energy corresponding to the $\nu = 9$ level of HF and initial angle variable θ distributed in the interval $[-\pi/4, 0]$. The dipole parameter were set to represent the HF dipole, $\eta = 0$ and $\xi = 0.0029$, while the field parameters are $\epsilon = 3$ and $\Omega = 8$. The unperturbed tori corresponding to the $\nu = 4$ and the $\nu = 9$ energy levels of HF, as well as the separatrix, are shown in dotted lines. We note that in the presence of the field, the deformed tori couples several energy levels with energies beyond that of the separatrix. Therefore, by suitably adjusting the duration of the field, trajectories can be lead to dissociation on such surviving tori. We tackle this problem in the following section.
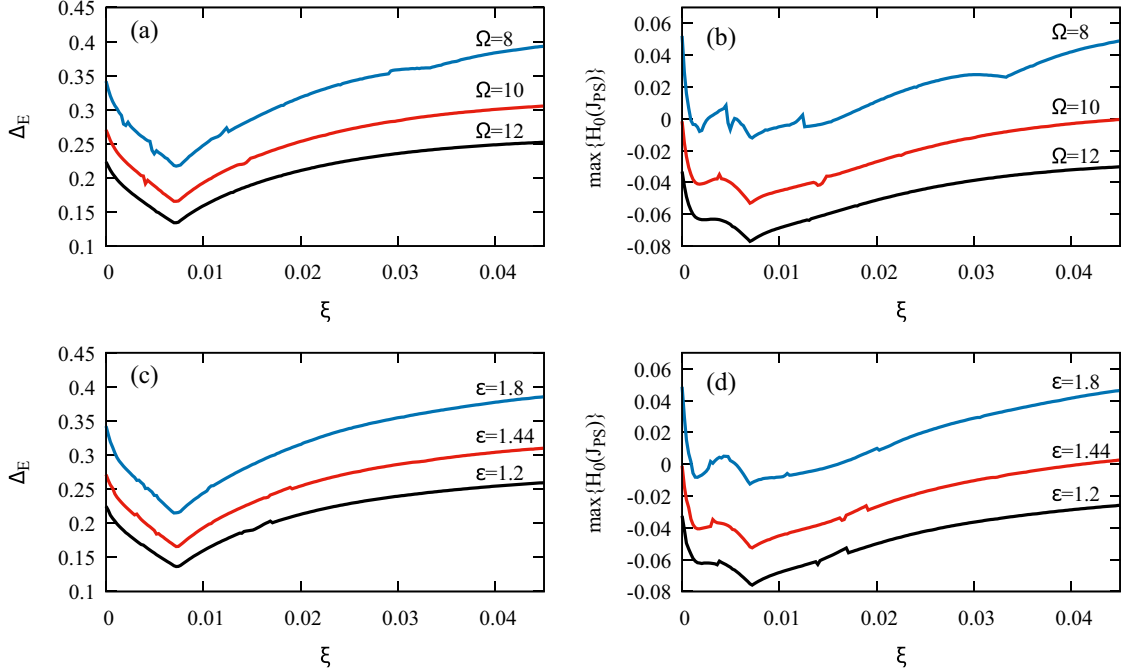
FIG. 1. (a) Energy inclination Δ_E and (b) maximum value of H_0 in the Poincaré surface of section as a function of the dipole range parameter ξ for $\epsilon = 1.6$. (c) Energy inclination Δ_E and (d) maximum value of H_0 in the Poincaré surface of section as a function of the dipole range parameter ξ for $\Omega = 9$. In all panels the initial energies were set to -0.162, which corresponds to the energy of the $\nu = 9$ vibrational level of the HF molecule and $\eta = 0$.

IV. PULSE-DRIVEN NONCHAOTIC DISSOCIATION

In order to design a field to perform the dissociation, we choose a laser pulse of the form

$$\mathcal{E}(t) = S(t)\varepsilon \sin(\Omega t), \qquad (18)$$

where $S(t)$ is a square envelope function,

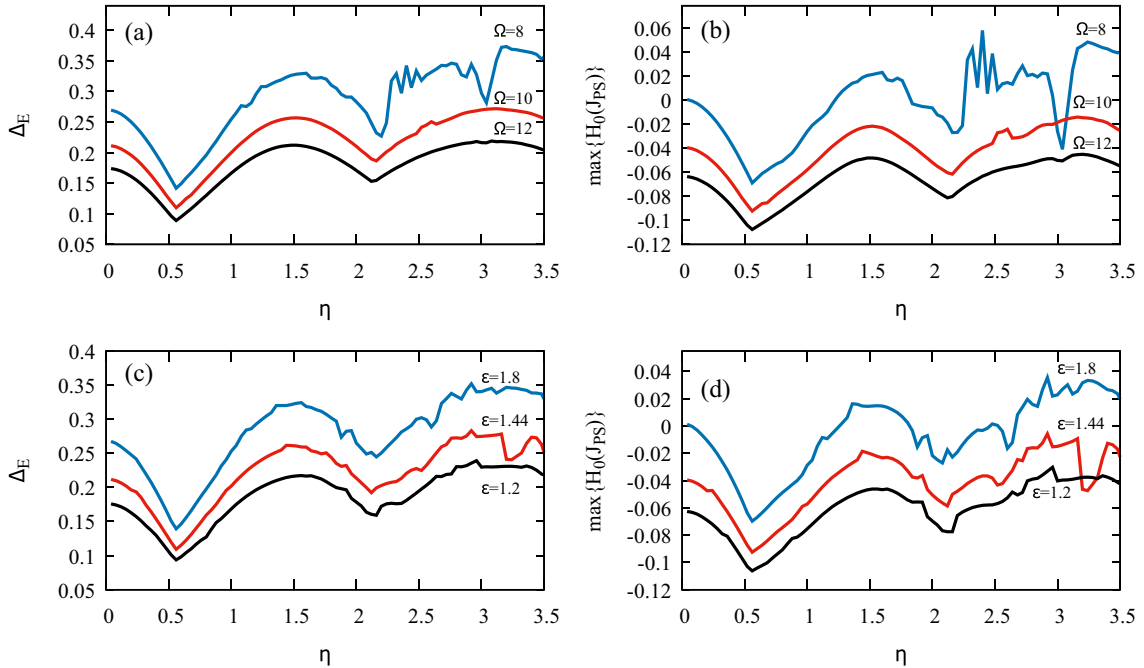$$S(t) = \begin{cases} 1, & 0 < t < t_p \\ 0, & \text{otherwise} \end{cases}. \qquad (19)$$

FIG. 2. (a) Energy inclination Δ_E and (b) maximum value of H_0 in the Poincaré surface of section as a function of the dipole oscillation parameter η for $\epsilon = 1.6$. (c) Energy inclination Δ_E and (d) maximum value of H_0 in the Poincaré surface of section as a function of the dipole oscillation parameter η for $\Omega = 9$. In all panels the initial energies were set to -0.162, which corresponds to the energy of the $\nu = 9$ vibrational level of the HF molecule and $\xi = 0.0029$.
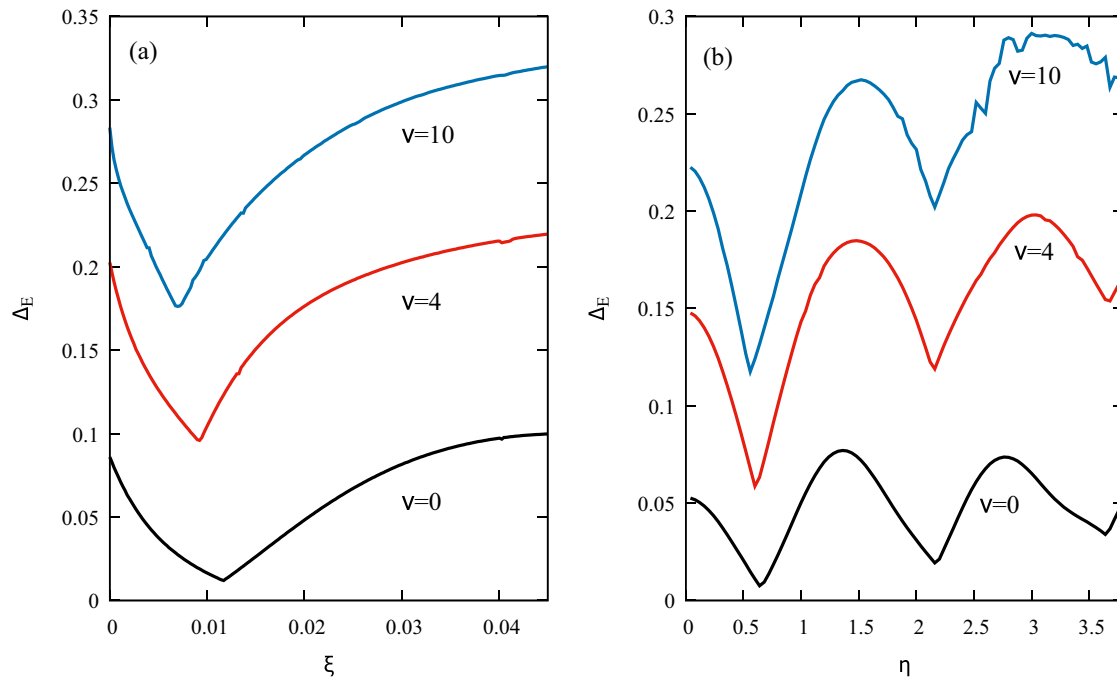
FIG. 3. Energy inclination Δ_E as a function of (a) ξ and (b) η for initial energies: -0.477 ($\nu = 0$), -0.317 ($\nu = 4$), and -0.138 ($\nu = 10$) and for field parameters: $\epsilon = 1.44$ and $\Omega = 9$.

The idea for performing a nonchaotic energy transition is the following: Consider that the initial conditions are placed in some lower energy region of a deformed torus. If the field is turned on at $t = 0$, then the trajectories will move on that torus, eventually raising their energy until they reach the higher energy region of the torus. At this moment, if the field is turned off, then the trajectories will remain with the higher energy. In particular, if the torus had crossed the separatrix of motion, then the trajectories will be dissociated.

The analysis of the energy inclinations and the corresponding maximum values of H_0 allows to select the possible values of frequency and amplitude of the field needed to perform the dissociation. For fixed field parameters, the energy inclination represents the possible gap in energy that a trajectory in the deformed torus can transverse. Once selected, the amplitude and the frequency, analyses of the torus deformation will give information about how the initial conditions should be distributed. Finally, it remains to set the duration of the
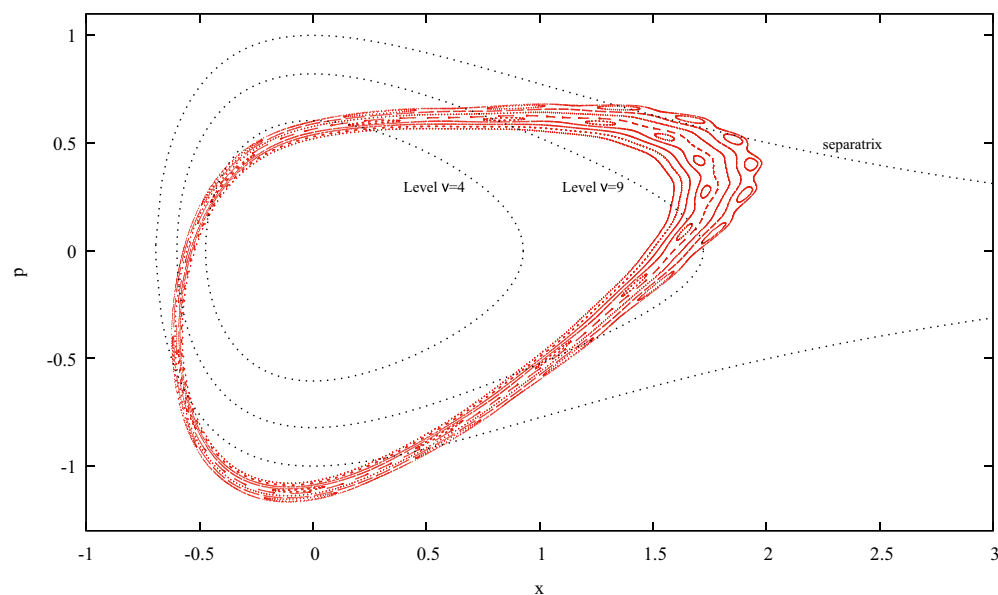

FIG. 4. Stroboscopic map for trajectories initially at the $\nu = 9$ level of HF and with initial angle variable $\theta \in [-\pi/4, 0]$ (red dots). The field parameters are $\epsilon = 3$ and $\Omega = 8$. The dipole parameters correspond to the HF molecule. The black dotted curves indicate the energy levels $\nu = 4$ and $\nu = 9$ and also the separatrix of motion in the absence of the field.
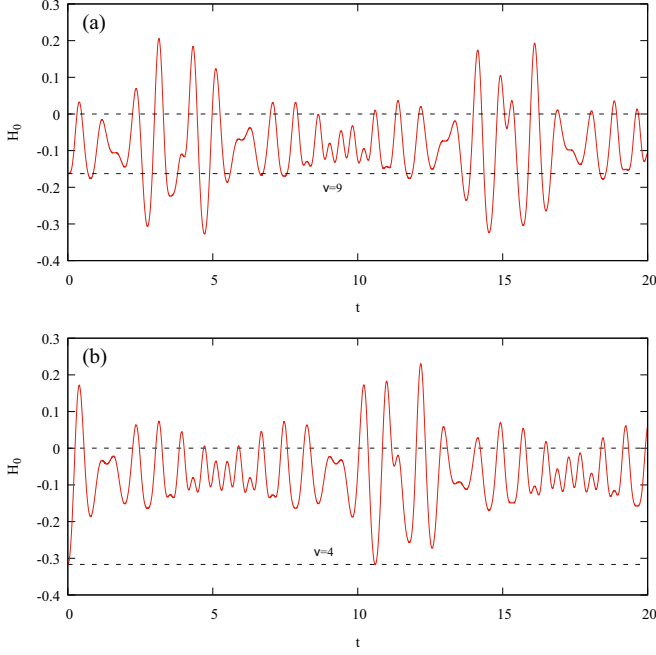
FIG. 5. Molecular Hamiltonian H_0 as a function of time for $\epsilon = 3$ and $\Omega = 8$. (a) Initial condition corresponding to the $\nu = 9$ level of HF and $\theta = 0$. (b) Initial condition corresponding to the $\nu = 4$ level and $\theta = 1.2\pi$.

external pulse, t_p. Direct calculation of $H_0(J)$ as a function of time provides the information about the pulse duration. In he following, we illustrate this methodology for the nonchaotic dissociation of the HF molecule.

Figure 5 shows the energy H_0 as a function of time for field parameters $\epsilon = 3$ and $\Omega = 8$ and for the dipole parameters of the HF molecule. In Fig. 5(a) the initial condition is set to the energy of the $\nu = 9$ level, while in Fig. 5(b) to the energy of the $\nu = 4$ level. The dotted lines indicate the energy levels and the dissociation threshold. Based on these panels, we can choose the appropriate duration of the pulses to perform the dissociation from the desired energy level.

Figure 6 illustrates the dissociation through deformed tori by showing the stroboscopic map for two sets of 100 trajectories. In both panels the field parameters are $\epsilon = 3$ and $\Omega = 8$ and the dipole parameters at those of the HF molecule. In Fig. 6(a) the trajectories are initially in the $\nu = 9$ torus distributed uniformly with initial angle variable $\theta \in [-\pi/4, \pi/4]$ (blue dots). At $t = 0$ the field is turned on, and at $t_p = 3.14$ the field is turned off. In Fig. 6(b), trajectories are initially in the $\nu = 4$ torus distributed with initial angle variable $\theta \in [\pi, 1.35\pi]$ (blue dots). At $t = 0$ the field is turned on and at $t_p = 0.39$ the field is turned off. Each panel shows the stroboscopic map for 10 periods of oscillation of the external field (the trajectories are taken at the times $t = 2\pi k/\Omega$, with $k = 0, \ldots, 10$). In case (a), the dissociation of all trajectories occurs in about four periods of the external field and in case (b) in about half of one period of the external field. In both cases the dissociation is carried out in a very regular fashion.
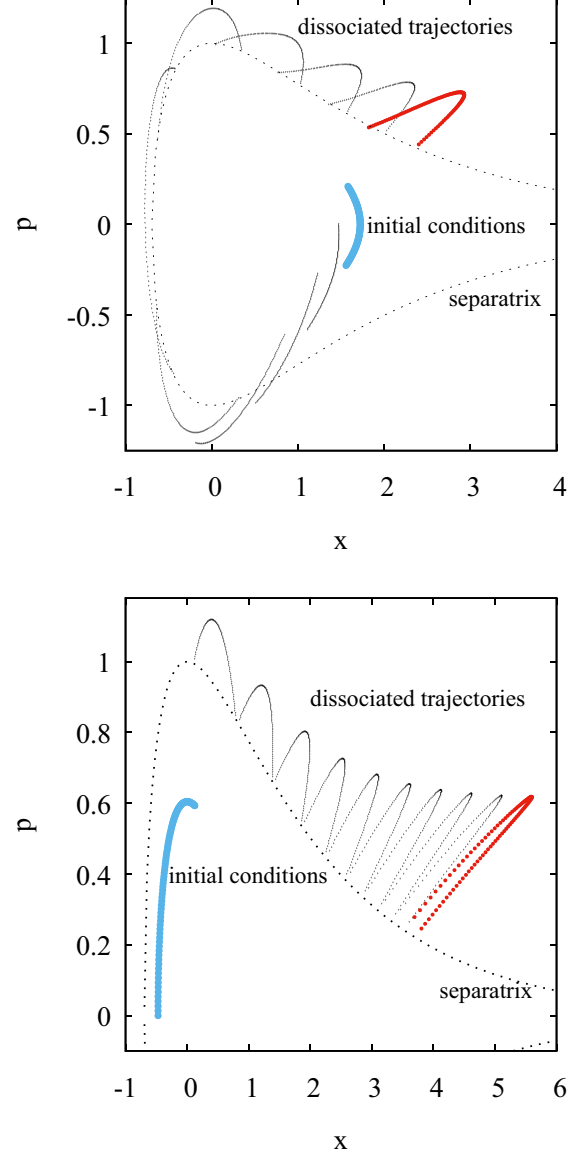

FIG. 6. (a) Stroboscopic map for an external pulse with $t_p = 3.14$ and for trajectories initially at the $\nu = 9$ level of HF and with initial angle variable $\theta \in [-\pi/4, \pi/4]$. (b) Stroboscopic map for a external pulse with $t_p = 0.39$ and for trajectories initially at the $\nu = 4$ level of HF and with initial angle variable $\theta \in [\pi, 1.35\pi]$. In both panels, the field parameters are $\epsilon = 3$ and $\Omega = 8$, the initial conditions are given by the blue points, and the trajectories at $t = 10$ periods of the external field are given by the red points (rightmost set of points above the separatrix).

We have also considered another envelope function for the external pulse in our calculations [31],

$$S'(t) = \begin{cases} \sin^2\left(\frac{\pi t}{2t_r}\right), & 0 < t < t_r \\ 1, & t_r < t < t_p - t_r \\ \cos^2\left[\frac{\pi(t - t_p + t_r)}{2t_r}\right], & t_p - t_r < t < t_p \\ 0, & \text{otherwise} \end{cases} \tag{20}$$

which ensures a smooth switch-on and switch-off of the pulse, with t_r being the rise-fall time of the pulse. We have obtained quite similar results with this envelope function, so these

results are not shown here. For example, using the same parameters of Fig. 6(a) of Fig. 6, the dynamics is essentially indistinguishable for $t_r < 0.1$. For increasing values of t_r, some trajectories become trapped in less energetic tori located in the bound region of the potential, leading to a decreasing number of dissociated trajectories. For $t_r = 0.2$, about 65% of the trajectories are dissociated. However, this can be compensated by increasing the field amplitude, e.g., setting $\epsilon = 4$ and $t_r = 0.2$, we again obtain a dissociation dynamics very close to that of the square pulse. Therefore, we have concluded that the technique can also be applied with alternatives envelope functions.

Finally, we discuss some practical aspects concerning the parameters used in our calculations (see Ref. [28] for the conversion factors). The field peak intensities considered here are of the order of 10^{15} W/cm^2, while the frequencies are in the range of few hundreds of nanometers (in the near ultraviolet range). This intensity is comparable to the ones considered in works which used monochromatic subpicosecond pulses and can be achieved in the laboratory [15,40], but it is two orders of magnitude larger than works that consider dissociation by means of chirped pulses [18,41]. The pulse durations considered in Figs. 6(a) and 6(b) are $t_p = 3.14$ (≈ 7 fs) and $t_p = 0.39$ (≈ 0.9 fs), respectively. Such ultrashort pulse, especially the subfemtosecond pulse, may be difficult to implement in practice [42]. However, this does not present a difficulty to our method since, instead of turning the field off at $t_p = 0.9$ fs, we could have left the trajectories in the deformed tori for longer times and still achieve nonchaotic dissociation. For instance, as can be seen in Fig. 5(b), we could have chosen $t_p = 12.17$ (≈ 27 fs), instead of $t_p = 0.39$, and still obtain similar results to those of Fig. 6(b).

V. CONCLUSIONS

In this work, we have investigated the deformations of surviving tori of the driven Morse oscillator as a function of the parameters of a harmonic laser field and dipole function. The main features of the dependence of the deformation on the amplitude and frequency of the field were captured by a formula obtained from perturbation theory and confirmed by numerical calculations: The deformation is large for increasing amplitude-frequency ratio. Additionally, surviving tori can be found more easily in the high-frequency regime, where the off-resonance condition is usually met and the chaotic regime can be avoided.

Apart from the field parameters, the deformation of a surviving torus depends also crucially on the initial energy and on the dipole parameters. For a given initial energy, the deformation presents a minimum at some given dipole range, whereas it can present relatively large values either for short- and long-range dipoles. The oscillatory character of the dipole also have an enormous influence on the deformations, with highly oscillatory dipoles presenting large deformations, even when the amplitude of the dipole is relatively small. These distinct behavior of the energy inclination with the range parameter and dipole oscillation parameter can be attributed to the coupling of the dipole with the unperturbed system expressed through the Fourier series expansion of the dipole in the angle variable of the system. Thus, changing a certain dipole parameter will affect the Fourier components and consequently the energy inclination.

From these results, we can conclude that, in the regime of high frequency and large field amplitudes, there exist deformed tori for a large set of dipole parameters which cross the separatrix of motion, allowing for the coupling between bound states with unbound states. In view of this fact, we have proposed the use of an appropriately designed laser pulse to perform the dissociation of trajectories on such surviving tori. We have illustrated the mechanism using the parameters of the HF molecule. We hope this work can stimulate investigations of the applicability of the proposed mechanism on related systems, such as the hydrogen atom and triatomic molecules [43,44].

[1] M. Bitter and V. Milner, Phys. Rev. Lett. **118**, 034101 (2017).

[2] J. Gong and P. Brumer, Annu. Rev. Phys. Chem. **56**, 1 (2005).

[3] R. C. Brown and R. E. Wyatt, Phys. Rev. Lett. **57**, 1 (1986).

[4] R. Jensen, S. Susskind, and M. Sanders, Phys. Rep. **201**, 1 (1991).

[5] M. J. Norman, C. Chandre, T. Uzer, and P. Wang, Phys. Rev. A **91**, 023406 (2015).

[6] R. M. O. Galvao, L. C. M. Miranda, and J. T. Mendonca, J. Phys. B **17**, L577 (1984).

[7] Y. Gu and J.-M. Yuan, Phys. Rev. A **36**, 3788 (1987).

[8] V. Constantoudis and C. A. Nicolaides, Phys. Rev. A **55**, 1325 (1997).

[9] V. Constantoudis and C. A. Nicolaides, Phys. Rev. E **64**, 056211 (2001).

[10] S. Huang, C. Chandre, and T. Uzer, J. Chem. Phys. **128**, 174105 (2008).

[11] V. Constantoudis and C. A. Nicolaides, J. Chem. Phys. **122**, 084118 (2005).

[12] M. Thachuk and D. M. Wardlaw, J. Chem. Phys. **102**, 7462 (1995).

[13] D. Poppe and J. Korsch, Physica D **24**, 367 (1987).

[14] R. B. Walker and R. K. Preston, J. Chem. Phys. **67**, 2017 (1977).

[15] M. E. Goggin and P. W. Milonni, Phys. Rev. A **37**, 796 (1988).

[16] R. Graham and M. Höhnerbach, Phys. Rev. A **43**, 3966 (1991).

[17] J.-M. Yuan and W.-K. Liu, Phys. Rev. A **57**, 1992 (1998).

[18] J.-H. Kim, W.-K. Liu, and J.-M. Yuan, J. Chem. Phys. **111**, 216 (1999).

[19] E. F. de Lima and M. A. M. de Aguiar, Phys. Rev. A **77**, 033406 (2008).

[20] A. Sethi and S. Keshavamurthy, Phys. Rev. A **79**, 033416 (2009).

[21] E. de Lima, E. Rosado, L. Castelano, and R. E. de Carvalho, Phys. Lett. A **378**, 2657 (2014).

[22] K. I. Dimitriou, V. Constantoudis, T. Mercouris, Y. Komninos, and C. A. Nicolaides, Phys. Rev. A **76**, 033406 (2007).

[23] R. Heather and H. Metiu, J. Chem. Phys. **88**, 5496 (1988).

[24] M. A. Buldakov, V. N. Cherepanov, E. V. Koryukina, and Y. N. Kalugina, J. Phys. B **42**, 105102 (2009).

[25] M. A. Buldakov and V. N. Cherepanov, J. Phys. B **37**, 3973 (2004).

[26] G. Gopakumar, M. Abe, M. Kajita, and M. Hada, Phys. Rev. A **84**, 062514 (2011).

[27] R. Guérout, M. Aymar, and O. Dulieu, Phys. Rev. A **82**, 042508 (2010).

[28] E. F. de Lima and R. E. de Carvalho, Physica D (Amsterdam) **241**, 1753 (2012).

[29] E. F. de Lima, T. N. Ramos, and R. E. de Carvalho, Phys. Rev. E **87**, 014901 (2013).

[30] W.-K. Liu, B. Wu, and J.-M. Yuan, Phys. Rev. Lett. **75**, 1292 (1995).

[31] W.-K. Liu, J.-M. Yuan, and S. H. Lin, Phys. Rev. A **60**, 1363 (1999).

[32] T. Topçu and F. Robicheaux, Phys. Rev. E **83**, 046607 (2011).

[33] T. Topçu and F. Robicheaux, J. Phys. B **43**, 205101 (2010).

[34] G. Murgida, D. Wisniacki, P. Tamborenea, and F. Borondo, Chem. Phys. Lett. **496**, 356 (2010).

[35] M. Forlevesi, R. E. de Carvalho, and E. de Lima, Physica A (Amsterdam) **490**, 681 (2018).

[36] A. J. Lichtenberg and M. A. Lieberman, *Regular and Stochastic Motion* (Springer-Verla New York, 1983), pp. xxi, 499.

[37] D. Richards, J. G. Leopold, and R. V. Jensen, J. Phys. B **22**, 417 (1989).

[38] A. Guldberg and G. D. Billing, Chem. Phys. Lett. **186**, 229 (1991).

[39] C. C. Rankin and W. H. Miller, J. Chem. Phys. **55**, 3150 (1971).

[40] S. Chelkowski and A. D. Bandrauk, Phys. Rev. A **41**, 6480 (1990).

[41] S. Chelkowski, A. D. Bandrauk, and P. B. Corkum, Phys. Rev. Lett. **65**, 2355 (1990).

[42] J. T. Lin, S. H. Lin, and T. F. Jiang, Phys. Rev. A **61**, 033407 (2000).

[43] A. Lopez-Pina, J. C. Losada, R. M. Benito, and F. Borondo, J. Chem. Phys. **145**, 244309 (2016).

[44] A. Sethi and S. Keshavamurthy, Mol. Phys. **110**, 717 (2012).